JOURNAL OF BACTERIOLOGY, Feb. 2008, p. 915–925 Vol. 190, No. 3
0021-9193/08/$08.00+0 doi:10.1128/JB.01647-07

The *Campylobacter jejuni* NADH:Ubiquinone Oxidoreductase (Complex I) Utilizes Flavodoxin Rather than NADH[▽]

Dilan R. Weerakoon and Jonathan W. Olson*

Department of Microbiology, North Carolina State University, Raleigh, North Carolina

Received 11 October 2007/Accepted 18 November 2007

Campylobacter jejuni **encodes 12 of the 14 subunits that make up the respiratory enzyme NADH:ubiquinone oxidoreductase (also called complex I). The two *nuo* genes not present in *C. jejuni* encode the NADH dehydrogenase, and in their place in the operon are the novel genes designated Cj1575c and Cj1574c. A series of mutants was generated in which each of the 12 *nuo* genes (homologues to known complex I subunits) was disrupted or deleted. Each of the *nuo* mutants will not grow in amino acid-based medium unless supplemented with an alternative respiratory substrate such as formate. Unlike the *nuo* genes, Cj1574c is an essential gene and could not be disrupted unless an intact copy of the gene was provided at an unrelated site on the chromosome. A *nuo* deletion mutant can efficiently respire formate but is deficient in α-ketoglutarate respiratory activity compared to the wild type. In *C. jejuni*, α-ketoglutarate respiration is mediated by the enzyme 2-oxoglutarate:acceptor oxidoreductase; mutagenesis of this enzyme abolishes α-ketoglutarate-dependent O_2 uptake and fails to reduce the electron transport chain. The electron acceptor for 2-oxoglutarate:acceptor oxidoreductase was determined to be flavodoxin, which was also determined to be an essential protein in *C. jejuni*. A model is presented in which CJ1574 mediates electron flow into the respiratory transport chain from reduced flavodoxin and through complex I.**

Campylobacter jejuni is the leading cause of human bacterial gastroenteritis, campylobacteriosis, in the world (1, 11, 21). Humans are infected by ingestion of contaminated food, typically poultry, where *C. jejuni* is a frequent resident (6, 11). The physiology of *C. jejuni* has adapted to take advantage of life in the lower avian cecum, where *C. jejuni* predominates (3). Anaerobic fermentation appears to be the dominant lifestyle in the cecum (20), and *C. jejuni* utilizes fermentation by-products such as small organic acids as both carbon and energy sources (18, 22, 23, 35, 38). *C. jejuni* itself is nonfermentative and uses oxidative phosphorylation for all its energy demands. The genome sequence of *C. jejuni* codes for respiratory components that can utilize multiple electron donors and acceptors in a branched electron transport chain (27). One of these components in *C. jejuni* is a proton pump called complex I, which is widely found in bacteria, archaea, and the mitochondria of eukaryotes (12). This complex (also called NADH:ubiquinone oxidoreductase) is the first enzyme in many respiratory chains and catalyzes the transfer of electrons from NADH to the quinone pool, coupled with the translocation of protons across a membrane (12). The fact that complex I occurs in the *C. jejuni* genome sequence was somewhat surprising, as it has been shown elsewhere that NADH is a poor respiratory electron donor (14).

The genes that code for complex I of most bacteria are clustered in a conserved order (30) consisting of 14 different genes that are designated either as *nuo* (*N*ADH:*u*biquinone *o*xidoreductase) (37) or as *nqo* (*N*ADH:*q*uinone *o*xidoreductase) (12, 40). Complex I has been well characterized in both *Escherichia coli* (4, 19) and *Paracoccus denitrificans* (39), and a model of the subunit structure and function has emerged. Of the 14 subunits, seven subunits (NuoA, NuoH, and NuoJ to NuoN) are integral membrane proteins and the remaining seven (NuoB to NuoG and NuoI) are peripheral subunits. The known redox cofactors are found in the peripheral subunits (12), including those of the NADH dehydrogenase fragment which has been localized to NuoE, NuoF, and NuoG (13). Like these model systems, the complex I genes of *C. jejuni* are organized in the 14-gene *nuo* operon; however, *nuoE* and *nuoF* are absent from this operon and are replaced with two genes (Cj1575c and Cj1574c) of unknown function (Fig. 1) (27). Since *nuoE* and *nuoF* encode the NADH dehydrogenase subunit, it is not surprising that NADH is not the donor to complex I of *C. jejuni*. The other 12 subunits of complex I in *C. jejuni* do contain sequence similarities to complex I subunits of other bacteria including *E. coli* and *P. denitrificans* (19, 39).

The electron donor to complex I of *C. jejuni* has yet to be identified. Finel has suggested that HP1264 and HP1265 (homologues to CJ1575 and CJ1574) in *Helicobacter pylori* may provide a docking site for a protein that may pass its electrons directly to NuoG (Nqo3) (9), and Myers and Kelly suggest a flavodoxin or ferredoxin as a possible candidate (24). Flavodoxins are small acidic proteins that are involved in electron transfer and contain one molecule of flavin mononucleotide (FMN) that acts as the redox active component (29), while ferredoxins are redox active iron-sulfur proteins classified by the number of Fe-S clusters (5). The genome sequence of *C. jejuni* codes for several ferredoxins and one flavodoxin (27). The genome also codes for two enzymes that typically use either ferredoxin or flavodoxin as the electron acceptor, pyruvate ferredoxin (flavodoxin) oxidoreductase (PFOR) and 2-oxoglutarate oxidoreductase (OOR). PFORs are iron-sulfur proteins involved in the coenzyme A (CoA)-dependent oxida-

* Corresponding author. Mailing address: Department of Microbiology, Campus Box 7615, North Carolina State University, Raleigh, NC 27695. Phone: (919) 515-7860. Fax: (919) 515-7867. E-mail: jwolson@ncsu.edu.

▽ Published ahead of print on 7 December 2007.

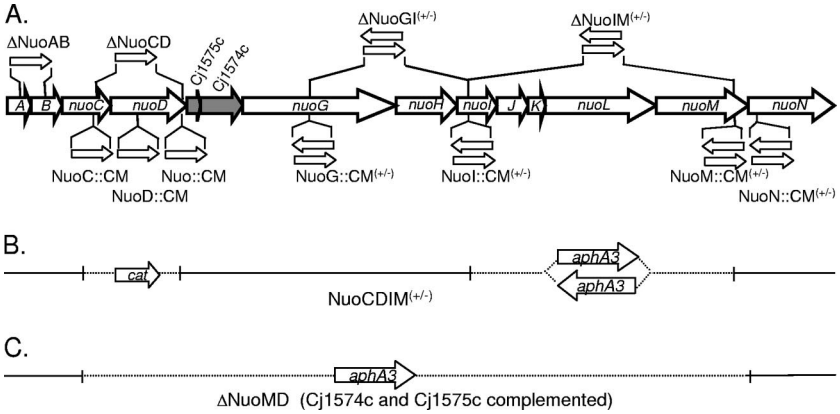

FIG. 1. Genetic organization of the *nuo* operon and graphical representation of mutants. (A) Deletions are indicated above the genes; sites of insertions are indicated below the genes. The arrow indicates the chloramphenicol resistance cassette *cat*; the direction of the arrow indicates the orientation of *cat* within the gene. (B) Representation of the deleted regions (dotted lines) in the double mutant ΔNuoCDIM$^+$. (C) Representation of the deleted region (dotted line) in ΔNuoMD.

tive decarboxylation of pyruvate to form acetyl-CoA (15, 28). OOR enzymes are involved in the decarboxylation of 2-oxoglutarate in the presence of CoA to form succinyl-CoA and CO_2 (16). In *C. jejuni*, PFOR is encoded by Cj1476c and codes for a single protein subunit while OOR is composed of four subunits encoded by the genes *oorDABC* (Cj0535 to Cj0538) (27). PFOR and OOR both play vital roles in central carbon metabolism in *C. jejuni*, serving the analogous functions of pyruvate dehydrogenase and α-ketoglutarate dehydrogenase, enzymes which are not found in the *C. jejuni* genome (27).

In this article, we demonstrate that complex I functions as a respiratory enzyme that accepts electrons from flavodoxin rather than NADH. We also show that OOR is responsible for α-ketoglutarate-dependent respiratory activity and that flavodoxin is the electron acceptor for this enzyme. Furthermore, we show that both Cj1574c and *fldA* (which encodes flavodoxin) are essential genes in *C. jejuni*. We suggest that flavodoxin is essential because of its role as a substrate for two important steps in central carbon metabolism and that CJ1575 and CJ1574 are essential in maintaining a pool of oxidized flavodoxin.

MATERIALS AND METHODS

Bacterial strains and growth conditions. *C. jejuni* strains are listed in Table 1. Cells were grown either on tryptic soy agar plates supplemented with 10% sheep blood (called BA plates) or in Mueller-Hinton (MH) broth. Formate (20 mM for liquid culture and 50 mM for plates), sodium nitrate (10 mM), chloramphenicol (25 μg/ml), and kanamycin (30 μg/ml) were added to the medium as indicated. *C. jejuni* was routinely cultured microaerobically at 37°C in a trigas incubator (model NU-4950; NuAire, Inc.), in which the gas composition was constantly maintained at 12% O_2 and 5% CO_2 and the balance N_2. *E. coli* strains are listed in Table 1. Luria-Bertani broth and agar supplemented with ampicillin (at 150 μg/ml), chloramphenicol (at 25 μg/ml), and kanamycin (at 30 μg/ml) were used for growing various *E. coli* strains, as noted.

Cloning and construction of *nuo* mutants. Oligonucleotide primers (Table 2) were designed using the genome sequence of *C. jejuni* NCTC 11168 (27) using the DNA analysis program MacVector. Unless otherwise stated, PCR amplification was performed with *Taq* DNA polymerase (Promega) using *C. jejuni* NCTC 11168 genomic DNA as a template. Genomic DNA was isolated using the MasterPure Complete DNA and RNA purification kit (Epicentre Biotechnologies). The PCR products were cloned into pBluescript II$^+$ KS (Stratagene) and pCR2.1 TOPO (Invitrogen) vectors and confirmed by restriction analysis (plasmids are listed in Table 3). The cloned *nuo* genes were then disrupted by insertion of a chloramphenicol acetyltransferase resistance cassette (*cat*), removed from pJMA-001 by SmaI digestion (pJMA-001 contains *cat* from plasmid pRY111 [41]), and cloned into the PvuII site of pGEM-T Easy (Promega) to yield plasmid pJMA-001. Double mutants were obtained by using a kanamycin resistance cassette, *aphA-3* (36). Insertion of the cassettes was confirmed by isolation of genomic DNA from the mutants and PCR amplification of the relevant *nuo* genes, followed by agarose gel electrophoresis to monitor the increase in size of the *nuo* genes due to the insertion of the cassettes (data not shown).

Transformation of *C. jejuni*. *C. jejuni* electrocompetent cells were made by harvesting cells by swab from BA plates and washing the cells three times in an ice-cold 9% sucrose and 15% glycerol solution. Cells were used immediately or frozen at −80°C for future use. For transformation, *C. jejuni* electrocompetent cells were incubated with 1 to 5 μg of plasmid DNA on ice for 10 min. The cells were then placed in a 2-mm electroporation cuvette and given a pulse of 2,500 V in an ECM399 electroporator (BTX, San Diego, CA), and 50 μl of MH broth was added to the cuvette and subsequently incubated on ice for 10 min. The cells were then spotted onto a cold BA plate supplemented with formate and sodium nitrate and incubated for 24 h in an anaerobic jar containing an Anaerobic BBL GasPak Plus with palladium catalyst (anaerobic pack). After 24 h on nonselective medium, the cells were transferred onto BA plates supplemented with chloramphenicol, formate, and sodium nitrate and incubated in an anaerobic jar with an anaerobic pack. Resistant colonies were selected after 3 to 5 days of incubation, and the colonies were screened for recombination of the interrupted version of the gene by PCR of genomic DNA using primers against the targeted gene.

Construction of the *nuo* merodiploid strains. pET7574 contains Cj1575c and Cj1574c in frame with a hexahistidine epitope tag. The *cat* cassette was then inserted into a BlpI restriction site located downstream of Cj1575c and Cj1574c in pET7574 to yield pET7574::CM. The coding region of the two genes and cassette was excised from pET7574::CM by digestion with BglII and StyI and treated with T4 DNA polymerase (Promega) to ensure blunt ends. This fragment was then cloned into the NdeI restriction site of pHydA (Table 3), which contains a 1,193-bp fragment of *hydA*, to yield pHyd7574::CM. Electrocompetent *C. jejuni* cells were transformed with pHyd7574::CM to obtain 7574MD. Δ74MD was constructed as follows: a 2,659-bp fragment of *nuoC*, *nuoD*, Cj1575c, Cj1574c, and *nuoG* was amplified by PCR using *C. jejuni* wild-type (WT) genomic DNA and primers NuoF and NuoR and cloned into pCR2.1-TOPO to yield pNuo. This plasmid was digested with SspI to create a deletion within Cj1574c, and *aphA-3* was inserted into the SspI sites of Cj1574c to yield pNuo::KAN. Restriction analysis revealed that *aphA-3* was in the same orientation as Cj1574c. This plasmid was then electroporated with competent 7574MD cells to obtain Δ74MD. PCR was carried out to confirm that *aphA-3* was inserted in the Cj1574c gene of the *nuo* operon and not in the Cj1574c gene cloned into *hydA*. ΔNuoMD was constructed as follows: *nuoN* was digested out of pNuoN (Table 3) via EcoRI, blunt ended with T4 DNA polymerase, and cloned into the BamHI site of pNuoCD (Table 3) in the same orientation as *nuoCD* to yield pNuoCDN. This plasmid was digested by creating two deletions between the AccB7I site of *nuoC* and the ClaI site of *nuoD* and the ClaI sites of *nuoD* and *nuoN*. Next, *aphA-3* was

TABLE 1. Strains used in this study

Strain	Description and orientation of antibiotic cassette if any[b]	Source
C. jejuni		
NCTC 11168	Parent strain for *C. jejuni* strains (WT)	NCTC[a]
ΔNuoAB	*cat* replaces *nuoA* and *nuoB* deletion	This study
NuoC::CM	*cat* inserted within *nuoC*	This study
NuoD::CM	*cat* inserted within *nuoD*	This study
ΔNuoCD	*cat* replaces *nuoC* and *nuoD* deletion	This study
Nuo::CM	*cat* inserted within *nuoD*	This study
NuoG::CM$^+$	Same-orientation *cat* inserted within *nuoG*	This study
NuoG::CM$^-$	Opposite-orientation *cat* inserted within *nuoG*	This study
ΔNuoGI$^+$	Same-orientation *cat* replaces *nuoG-to-nuoI* deletion	This study
ΔNuoGI$^-$	Opposite-orientation *cat* replaces *nuoG-to-nuoI* deletion	This study
NuoI::CM$^+$	Same-orientation *cat* inserted within *nuoI*	This study
NuoI::CM$^-$	Opposite-orientation *cat* inserted within *nuoI*	This study
ΔNuoIM$^+$	Same-orientation *cat* replaces *nuoI-to-nuoM* deletion region	This study
ΔNuoIM$^-$	Opposite-orientation *cat* replaces *nuoI-to-nuoM* deletion region	This study
NuoM::CM$^+$	*cat* inserted within *nuoM*	This study
NuoM::CM$^-$	*cat* inserted within *nuoM*	This study
ΔNuoCDIM$^+$	*cat* replaces *nuoC-nuoD* deletion; same-orientation *aphA-3* replaces *nuoI-to-nuoM* deletion	This study
ΔNuoCDIM$^-$	*cat* replaces *nuoC-nuoD* deletion; opposite-orientation *aphA-3* replaces *nuoI-to-nuoM* deletion	This study
NuoN::CM$^+$	Same-orientation *cat* inserted within *nuoM*	This study
NuoN::CM$^-$	Opposite-orientation *cat* inserted within *nuoM*	This study
7574MD	Cj1575c and Cj1574c merodiploid strain	This study
Δ74MD	*aphA-3* inserted within Cj1574c in the *nuo* operon in 7574MD	This study
ΔNuoMD	*aphA-3* inserted between *nuoC* and *nuoN* in 7574MD	This study
FldMD	*fldA* merodiploid strain	This study
FldMD::CM	*cat* inserted within *fldA* (Cj1382c) in FldMD	This study
OorB::CM	*cat* inserted within *oorB* (Cj0537)	This study
FdxA::CM	*cat* inserted within *fdxA* (Cj0333c)	This study
0369::CM	*cat* inserted within Cj0369c	This study
E. coli		
DH5α	Cloning strain	Lab stock
BL21 Rosetta	Expression strain	Lab stock
GM2163	*dam*-negative strain	New England Biolabs

[a] NCTC, National Collection of Type Cultures.
[b] "Same" and "opposite" orientations mean that *cat* or *aphA-3* is in the same or opposite orientation relative to the gene, respectively.

inserted into the AccB7I/ClaI site to yield pΔNuoCDN::KAN. Restriction analysis revealed that *aphA-3* was in the same orientation as *nuoC* and *nuoN*. This plasmid was mobilized via electroporation into competent 7574MD cells to obtain ΔNuoMD.

Construction of the flavodoxin merodiploid strains. A merodiploid flavodoxin strain (FldMD) was constructed as follows: primers designed to engineer an NdeI site to the first codon of the *fldA* gene (Cj1382c) (FldProF) and a XhoI site in place of the stop codon of *fldA* (FldProR) and platinum *Pfu* polymerase (Invitrogen) were used to amplify *fldA* using *C. jejuni* WT genomic DNA and cloned into pCR2.1-TOPO to yield pTOPOFld. *fldA* was excised from pTOPOFld by digestion with NdeI and XhoI and then cloned into the NdeI/XhoI-digested pET-21a(+) in frame with the hexahistidine tag to yield pETFld. *aphA-3* was then inserted into the BlpI site of pETFld to yield pET7574::KAN. *fldA* and *aphA-3* were then cut out of pET7574::KAN using BglII and StyI, blunt ended with T4 DNA polymerase, and cloned into the NdeI site of pHydA to yield pHydFld::KAN. This plasmid was used to transform competent *C. jejuni* to obtain FldMD. FldMD::CM was constructed as follows: the *fldA* gene (Cj1382c) and two flanking regions of 948 bp upstream of the start codon and 287 bp downstream of the stop codon, respectively, were amplified by PCR using *C. jejuni* WT genomic DNA and primers FldF and FldR, blunt ended with T4 DNA polymerase, and phosphorylated with T4 polynucleotide kinase (Promega). This product was then cloned into the EcoRV site of pBluescript II KS(+), where the EcoRI restriction site has been destroyed (pKSΔRI), to yield pΔRIFld. The *cat* cassette was then cloned into the EcoRI site of pΔRIFld. The resulting plasmid, pΔRIFld::CM, was then electroporated into competent FldMD cells to obtain FldMD::CM. PCR was carried out to confirm that the original *fldA* gene in the genome contained the *cat* and not the *fldA* gene cloned into *hydA*.

Cloning of *oorB* and construction of OorB::CM. The *oorB* (Cj0537) gene was amplified by PCR using the primers OorF and OorR and cloned into pCR2.1-TOPO to yield pOorB. This plasmid was digested with SspI to create a deletion within *oorB*, and a *cat* cassette was then inserted into the SspI sites of this plasmid to obtain pOorB::CM. This plasmid was electroporated into competent WT *C. jejuni* cells to obtain OorB::CM. Restriction analysis revealed that the *cat* cassette was in the same orientation as the *oorB* gene.

qRT-PCR. Quantitative reverse transcriptase PCR (qRT-PCR) was performed using the QuantiTect Sybr green RT-PCR kit (Qiagen, Valencia, CA). RNA was extracted from *C. jejuni* cells grown to mid-log phase by using the MasterPure Complete DNA and RNA purification kit (Epicentre Biotechnologies).

The RT-PCR mixture included 40 ng RNA, 2 μM (each) of the forward and reverse primers, 1× QuantiTect Sybr green RT-PCR Master Mix (Qiagen), and 0.2 μl/reaction mixture QuantiTect reverse transcriptase mix (Qiagen). The reverse transcriptase reaction mixture was held at 50°C for 30 min, followed by a PCR initial activation step for 15 min at 95°C. The mixtures were then amplified for 30 cycles consisting of 94°C for 15 seconds, 60°C for 30 seconds, and 72°C for 30 seconds in an automated thermal cycler (Bio-Rad iCycler; Hercules, CA). The iCycler software was used to determine the threshold cycle for when each transcript could be detected. Threshold cycles were then compared to a standard curve, which was generated independently for each gene, to determine the number of starting RNA molecules. Total RNA in each sample was normalized by standardizing the copy number of that gene to that of an internal control, *gyrA* (Cj1027c).

Flavodoxin expression, purification, and characterization. *E. coli* strain BL21 Rosetta (Novagen) was transformed with pETFld. A 5-ml overnight culture of pETFld Rosetta grown at 37°C in Luria-Bertani broth supplemented with ampicillin was used to inoculate a fresh 500-ml Luria-Bertani broth. This inoculated culture was shaken at 37°C. When the optical density of the culture at 600 nm (OD_{600}) was between 0.5 and 0.7, the culture was induced with a final concentration of 0.5 mM IPTG (isopropyl-β-D-thiogalactopyranoside). Two hours

TABLE 2. Primers used in this study[a]

Primer	Description
NuoABF	5′-AAAAATCCTATGAGTTAAGCGGAG-3′
NuoABR	5′-AGTTTTCAAAAGCGGATGTCC-3′
NuoCF	5′-CGCAAAGAAAAAGCAAGTCGC-3′
NuoCR	5′-AAATCAAGCATAACCCCGCC-3′
NuoDF	5′-TGATTGGTTTGGACATCCGC-3′
NuoDR	5′-AAAGCAAGCACTTCGCCTGC-3′
NuoF	5′-ATGAAGTGCCAAAAGGTGGTC-3′
NuoR	5′-AATGTTTATGTGGTTTATGCGTGTC-3′
NuoGF	5′-GCATAAACCACATAAACATTGGGG-3′
NuoGR	5′-CAAATCACAAATCATAGCCACACC-3′
NuoIF	5′-TTATGGAACGGAGTATTCGGG-3′
NuoIR	5′-GCCAAAAAAGCCTAAAACCACTAC-3′
NuoMF	5′-CCACTTCATACTTGGGCACCTAAG-3′
NuoMR	5′-GAAATAGCATTATCACTTCCACGC-3′
NuoNF	5′-CTTCATACTTGGGCACCTAAGG-3′
NuoNR	5′-CACAAAGAACAAAAATCATCACTCC-3′
HydF	5′-GTTTAGAAAAAAAATACATCCACGC-3′
HydR	5′-CATAGGCTCTTCAAAAGGTCCC-3′
1575F	5′-CGCATATGAGAAGGGTAGATTTAAGA AAAAGC-3′
1574R	5′-GGCTCGAGTTTTGCTTCCTTTATGCGA ATTG-3′
FldProF	5′-GGCATATGTCAGTAGCAGTAATCTATG GT-3′
FldProR	5′-CCCTCGAGAGCAAAATAAGGTTTGATT TGTTC-3′
FldF	5′-GGTGCTAAAAAAATAGAACACTGGG-3′
FldR	5′-TGCTCAAAAAATCACAACTTCAGC-3′
OorF	5′-TCCGTCCGATTACTCTTTATCCAG-3′
OorR	5′-CCTCCTTCTTTTACACCCCCAC-3′
FdxF	5′-TACTCTCAGCAAAATCAGCCC-3′
FdXR	5′-TTGGATAAAAGAATACTACCGCTC-3′
0369F	5′-CTGCTTTGATTTTTTCTTGTCTGG-3′
0369R	5′-CACAGTCCTCACCACCTTTCT-3′
GyrAF-RT	5′-TGGTTGTAACTATCACACATCGTGG-3′
GyrAR-RT	5′-AATCATCATCATAAGTCGTAACGGC-3′
NuoHF-RT	5′-CACCTTTGATTTCTGCTATTTGTGC-3′
NuoHR-RT	5′-AAGTCCTGAAGTGCCGATGAC-3′
1574F-RT	5′-TGACGGGTTAGTGCTTTTTAGAG-3′
1574R-RT	5′-TCATTTTGCTTCCTTTATGCG-3′

[a] All primers came from Integrated DNA Technologies, Coralville, IA.

postinduction the cells were harvested by centrifugation, washed two times with lysis buffer (50 mM NaH_2PO_4, 300 mM NaCl, 10 mM imidazole), and resuspended with 40 ml lysis buffer. The cells were then broken by passage through a French pressure cell (Thermo Spectronic) three times at 20,000 lb/in^2. The crude extract was cleared by centrifugation at 12,000 × *g* for 5 min. The supernatant was collected and passed over a Ni-nitrilotriacetic acid agarose (5-ml bed volume) column (Qiagen) preequilibrated with lysis buffer. The column was then washed with 5 column volumes of wash buffer (50 mM NaH_2PO_4, 300 mM NaCl, 20 mM imidazole). Protein was eluted with elution buffer (50 mM NaH_2PO_4, 300 mM NaCl, 250 mM imidazole), and 2-ml fractions were collected. Elution fractions were assayed for protein by sodium dodecyl sulfate-polyacrylamide gel electrophoresis (SDS-PAGE) as described by Laemmli (17). Protein-containing fractions were dialyzed overnight in a 1-liter solution of 10 mM Tris, 10 mM NaCl, 1 mM dithiothreitol, and 10% glycerol at 4°C. Spectra were obtained using this purified flavodoxin in a Shimadzu UV-1650PC spectrophotometer. Spectra from commercially purchased FMN (MP Biomedicals, Inc.) and flavin adenine dinucleotide (FAD; Alexis Biochemicals) were used to compare the flavodoxin spectrum.

Cytochrome reduction assays. Cells were harvested with a swab into N_2-sparged phosphate-buffered saline (PBS), washed once, and sonicated in sealed tubes under N_2 to obtain cell extracts (CE). One milliliter each of CE was put into two quartz cuvettes, which were subsequently sealed with rubber stoppers, flushed with N_2 gas for 3 min, and then placed in a Shimadzu UV-1650PC spectrophotometer. A baseline spectrum was produced first without the addition of any substrates and second with the simultaneous addition of a 5 mM final concentration of α-ketoglutarate and a 0.5 mM final concentration of CoA. Protein concentrations were determined with the bicinchoninic acid protein assay kit (Pierce).

Reduction of flavodoxin. Purified flavodoxin and *C. jejuni* CE were mixed in a 4:1 ratio in a capped quartz cuvette to obtain a total volume of 1 ml; a blank cuvette contained only *C. jejuni* CE and buffer. The cuvettes were flushed with N_2 for 3 min and placed in a Shimadzu UV-1650PC spectrophotometer. A baseline spectrum was produced without the addition of substrate to verify the characteristic flavodoxin spectra. Next, a mixture of α-ketoglutarate and CoA was added to both quartz cuvettes simultaneously to give a final concentration of 5 mM and 0.5 mM, respectively. The cuvettes were inverted several times, and a spectral analysis was conducted immediately, 1 min, and 5 min after the addition of these substrates. To determine the flavodoxin reduction kinetics, the absorbance at 460 nm was monitored following addition of α-ketoglutarate and CoA.

Oxygen uptake experiments. O_2 was quantified using a YSI Model 5300 biological oxygen monitor (Yellow Springs Instrument Co., Yellow Springs, OH) and a Clark-type electrode. The electrode was inserted into a 5-ml-capacity glass chamber that was continuously stirred. Five milliliters of whole cells or CE was added to the chamber and allowed to equilibrate until no change in dissolved O_2 was observed for several minutes. Upon equilibration, substrate was added through a capillary tube via a Hamilton syringe into the chamber and the dissolved O_2 was recorded by chart recorder. After each experiment the chamber was calibrated using known concentrations of dissolved O_2. Substrate concentrations used were as follows: α-ketoglutarate and CoA, 5 mM and 0.5 mM, respectively; formate, 5 mM; NADH, 5 mM; NADPH, 5 mM.

SDS-PAGE and immunoblotting. To prepare membrane particles, 10 plates of each strain were harvested with a sterile swab into cold PBS, washed twice with PBS, and resuspended to 10 ml in cold PBS. The cells were broken by passage three times through a French pressure cell at 20,000 lb/in^2, and the lysate was cleared of unbroken cells by centrifugation at 12,000 × *g* for 5 min. The cleared supernatant was then subjected to fractionation by ultracentrifugation (150,000 × *g* for 90 min) in a Beckman L8-55 ultracentrifuge to isolate the membranes. The supernatant (soluble fraction) was saved for immunoblotting. The membrane fraction was washed once by resuspension in 10 ml cold PBS by Dounce homogenization, followed by centrifugation (150,000 × *g* for 90 min), and finally resuspended with a Dounce homogenizer. Ten micrograms of the soluble and membrane fractions was subjected to SDS-PAGE and transferred electrophoretically onto 0.2-μm nitrocellulose membranes (Bio-Rad Laboratories). The membranes were incubated in blocking solution (5% nonfat dry milk powder in Tris-buffered saline) for 30 min at room temperature. The primary antibody (purified mouse monoclonal tetra-His antibody [Qiagen]) was diluted 1:2,000 in blocking solution and incubated overnight at 4°C. The membranes were washed three times for 5 min each time with Tris-buffered saline and then incubated with a 1:3,000 dilution of purified goat anti-mouse–alkaline phosphatase conjugate antibody (Bio-Rad Laboratories) for 2 hours at room temperature. The membranes were washed twice with Tris-buffered saline, and a final wash was conducted with alkaline Tris buffer (100 mM Tris [pH 9.5], 100 mM NaCl, 50 mM $MgCl_2$). After washing, the membranes were developed with the alkaline phosphatase color development reagents 5-bromo-4-chloro-3-indoyl phosphate *p*-toluidine salt and *p*-nitroblue tetrazolium chloride purchased from Bio-Rad Laboratories.

RESULTS

Twelve *nuo* genes of complex I are dispensable. Twelve of the 14 genes in the complex I operon were disrupted via either an insertion or a deletion mutation (Fig. 1A). ΔNuoAB contains a deletion comprising 34% of *nuoA* and 53% of *nuoB*; the deleted DNA was replaced with *cat* (41). *nuoC* was disrupted both by an insertion with *cat* within the coding region (NuoC::CM) and also as part of a deletion comprising *nuoC* (15% deletion) and *nuoD* (99% deletion) to obtain ΔNuoCD. Two *nuoD* mutants were isolated with *cat* insertions near the middle (NuoD::CM) and near the end (Nuo::CM) of the gene. *nuoG* was disrupted by insertion of *cat* (in both orientations) within the coding region, and the resulting mutants were designated NuoG::CM$^+$ and NuoG::CM$^-$ (for all mutants, a superscript plus sign indicates that the cassette is transcribed in the same orientation as the gene and a superscript minus sign indicates cassette transcription opposite the gene). *nuoG* was

TABLE 3. Plasmids used in this study

Plasmid	Description[a]	Source
pCR2.1-TOPO	Cloning vector	Invitrogen
pBluescript II KS(+)	Cloning vector	Stratagene
pJMA-001	pGEM-T containing *cat* insert	Jay Andrus
pHP1	*aphA-3*-containing construct	David McGee
pET-21a(+)	Cloning vector	Novagen
pKSΔRI	pBluescript II KS(+) with destroyed EcoRI recognition site	This study
pNuoAB	*nuoA* and *nuoB* cloned from WT into EcoRV-digested pBluescript II KS(+)	This study
pKSΔNuoAB::CM	*cat* inserted into StyI- and BclI-digested pNuoAB	This study
pNuoC	*nuoC* cloned from WT into pCR2.1-TOPO	This study
pNuoC::CM	*cat* inserted into AccB7I-digested pNuoC	This study
pNuoD	*nuoD* cloned from WT into pCR2.1-TOPO	This study
pNuoD::CM	*cat* inserted into BsaMI-digested pNuoD	This study
pNuoCD	*nuoC* and *nuoD* cloned from WT into pCR2.1-TOPO	This study
pΔNuoCD::CM	*cat* inserted into AccB7I- and ClaI-digested pNuoCD	This study
pNuo	*nuoC*, *nuoD*, Cj1575c, Cj1574c, and *nuoG* cloned from WT into pCR2.1-TOPO	This study
pNuo::CM	*cat* inserted into ClaI-digested pNuo	This study
pNuoG	*nuoG* cloned from WT into pCR2.1-TOPO	This study
pNuoG::CM$^+$	Same-orientation *cat* inserted into Eco47III-digested pNuoG	This study
pNuoG::CM$^-$	Opposite-orientation *cat* inserted into Eco47III-digested pNuoG	This study
pNuoGI	*nuoG*, *nuoH*, and *nuoI* cloned from WT into pCR2.1-TOPO	This study
pΔNuoGI::CM$^+$	Same-orientation *cat* inserted into Eco47III-digested pNuoGI	This study
pΔNuoGI::CM$^-$	Opposite-orientation *cat* inserted into Eco47III-digested pNuoGI	This study
pNuoI	*nuoI* cloned from WT into pCR2.1-TOPO	This study
pNuoI::CM$^+$	Same-orientation *cat* inserted into Eco47III-digested pNuoI	This study
pNuoI::CM$^-$	Opposite-orientation *cat* inserted into Eco47III-digested pNuoI	This study
pNuoIM	*nuoI*, *nuoJ*, *nuoK*, *nuoL*, and *nuoM* cloned from WT into pCR2.1-TOPO	This study
ΔNuoIM::CM$^+$	Same-orientation *cat* inserted into Eco47III-digested pNuoIM	This study
pΔNuoIM::CM$^-$	Opposite-orientation *cat* inserted into Eco47III-digested pNuoIM	This study
pNuoM	*nuoM* cloned from WT into pCR2.1-TOPO	This study
pNuoM::CM$^+$	Same-orientation *cat* inserted into Eco47III-digested pNuoM	This study
pNuoM::CM$^-$	Opposite-orientation *cat* inserted into Eco47III-digested pNuoM	This study
pΔNuoIM::KAN$^+$	Same-orientation *aphA-3* inserted into Eco47III-digested pNuoIM	This study
pΔNuoIM::KAN$^-$	Opposite-orientation *aphA-3* inserted into Eco47III-digested pNuoIM	This study
pNuoN	*nuoN* cloned from WT into pCR2.1-TOPO	This study
pNuoN::CM$^+$	Same-orientation *cat* inserted into ClaI-digested pNuoN	This study
pNuoN::CM$^-$	Opposite-orientation *cat* inserted into ClaI-digested pNuoN	This study
pTOPO7574	Cj1575c and Cj1574c cloned from WT into pCR2.1-TOPO	This study
pET7574	Cj1575c and Cj1574c from pTOPO7574 inserted into NdeI/XhoI-digested pET-21a(+)	This study
pET7574::CM	*cat* inserted into BlpI-digested pET7574	This study
pHydA	*hydA* cloned from WT into pCR2.1-TOPO	This study
pHyd7574::CM	Cj1575c, Cj1574c, and *cat* inserted into NdeI-digested pHydA	This study
pNuo::KAN	*aphA-3* inserted into SspI-digested pNuo	This study
pNuoCDN	*nuoN* from pNuoN inserted into BamHI-digested pNuoCD	This study
pΔNuoCDN::KAN	*aphA-3* inserted into AccB7I- and ClaI-digested pNuoCDN	This study
pTOPOFld	*fldA* cloned from WT into pCR2.1-TOPO	This study
pETFld	*fldA* from pTOPOFld inserted into NdeI/XhoI-digested pET-21a(+)	This study
pETFld::KAN	*aphA-3* inserted into BlpI-digested pETFld	This study
pHydFld::KAN	*fldA* and *aphA-3* inserted into NdeI-digested pHydA	This study
pΔRIFld	*fldA* cloned from WT into EcoRV-digested pKSΔRI	This study
pΔRIFld::CM	*cat* inserted into EcoRI-digested pΔRIFld	This study
pOorB	*oorB* cloned from WT into pCR2.1-TOPO	This study
pOorB::CM	*cat* inserted into SspI-digested pOorB	This study
pFdxA	*fdxA* (Cj0333c) cloned from WT into pCR2.1-TOPO	This study
pFdxA::CM	*cat* inserted into BsaMI-digested pFdxA	This study
p0369	Cj0369c cloned from WT into pCR2.1-TOPO	This study
p0369::CM	*cat* inserted into BsaMI-digested p0369	This study

[a] "Same" and "opposite" orientations mean that *cat* or *aphA-3* is in the same or opposite orientation relative to the gene, respectively.

also disrupted as part of a deletion comprising *nuoG* (56% deletion), *nuoH*, and *nuoI* (23% deletion) to obtain ΔNuoGI$^+$ and ΔNuoGI$^-$. *nuoI* was disrupted by insertion of *cat* (in both orientations) within the coding region (NuoI::CM$^+$ and NuoI::CM$^-$) and also as part of a deletion comprising 77% of *nuoI*; all of *nuoJ*, *nuoK*, and *nuoL*; and 89% of *nuoM* to obtain ΔNuoIM$^+$ and ΔNuoIM$^-$. *nuoN* was disrupted by insertion of *cat* (in both orientations) to obtain NuoN::CM$^+$ and NuoN::CM$^-$. Two versions of a double mutant were obtained (Fig. 1B), using ΔNuoCD as the parent strain and insertion of *aphA-3* (in both orientations) into a deleted region consisting of *nuoI*, *nuoJ*, *nuoK*, *nuoL*, and *nuoM*, to yield ΔNuoCDIM$^+$ and ΔNuoCDIM$^-$. Each of these mutants was isolated on BA plates supplemented with formate (50 mM) and nitrate (10 mM) under an anaerobic atmosphere created by a GasPak Plus anaerobic pouch. All *nuo* mutants display similar growth

TABLE 4. Generation times of various strains in MH broth and MH broth plus 20 mM formate

Strain	Generation time (h) under condition:	
	MH plus formate	MH
WT	1.59	2.48
7475MD	1.31	1.90
NuoAB::CM	1.51	NG[a]
NuoC::CM	1.43	NG
NuoD::CM	1.57	NG
Nuo::CM	1.36	NG
NuoG::CM$^+$	1.33	NG
NuoG::CM$^-$	1.59	NG
NuoI::CM$^+$	1.62	NG
NuoI::CM$^-$	1.59	NG
NuoM::CM$^+$	1.73	NG
NuoM::CM$^-$	1.29	NG
NuoN::CM$^+$	1.60	NG
NuoN::CM$^-$	1.52	NG
ΔNuoCD	1.71	NG
ΔNuoGI$^+$	1.48	NG
ΔNuoGI$^-$	1.49	NG
ΔNuoIM$^+$	1.70	NG
ΔNuoIM$^-$	1.45	NG
ΔNuoCDIM$^+$	1.78	NG
ΔNuoCDIM$^-$	1.52	NG
Δ74MD	1.32	NG
ΔNuoMD	1.25	NG

[a] NG, no growth (cultures failed to double twice in 30 h).

phenotypes: they will not grow in liquid culture (cultures fail to double twice in 30 h) or on plates (no isolated colonies) unless the medium is supplemented with an alternative respiratory substrate such as formate. When formate is provided, these mutants displayed growth rates similar to that of the WT (Table 4; Fig. 2). Growth is entirely dependent on formate in these strains, which is shown graphically for strain ΔNuoMD in Fig. 2. Final culture OD_{600} is proportional to the initial concentration of formate (10 mM-supplemented cultures grow to a final OD_{600} of 0.18; 20 mM-supplemented cultures grow to a value of 0.36), and after the formate has been consumed growth ceases.

Expression of Cj1574c is required for viability. Despite many attempts, we were unsuccessful at mutating Cj1574c via either an insertion or a deletion mutation. We also noticed that *nuo* genes upstream of Cj1574c could be mutated only with *cat*

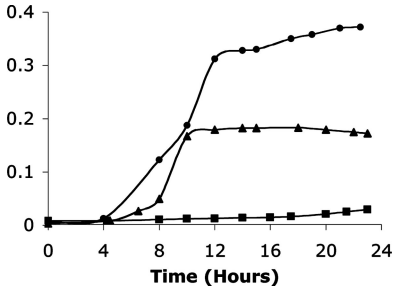

FIG. 2. Growth curve of ΔNuoMD in MH broth in a microaerobic atmosphere (5% CO_2, 12% O_2, balance N_2). Conditions: unsupplemented MH broth (squares), MH broth plus 10 mM formate (triangles), and MH broth plus 20 mM formate (circles). The *y* axis is in a linear scale to show the difference in the terminal optical density.

TABLE 5. Transcription of *nuoH* and Cj1574c in various strains as measured by qRT-PCR

Strain	Transcript abundance[a]	
	nuoH	Cj1574c
WT	2,410 ± 1,260	1,146 ± 220
NuoG::CM$^+$	288 ± 33	ND[b]
NuoG::CM$^-$	49 ± 11	ND
Δ74MD	29 ± 11	ND
ΔNuoMD	ND	3,250 ± 302

[a] Expressed as mRNA copies/ng total RNA ± standard deviation.
[b] ND, not determined.

that was in the same orientation as the *nuo* genes, while genes downstream of Cj1574c could be mutated with *cat* in either orientation (Fig. 1). qRT-PCR reveals that expression of the genes downstream of *cat* is affected differentially depending on the *cat* orientation. To show this effect quantitatively, we measured the transcription of *nuoH* in NuoG::CM$^+$ and NuoG::CM$^-$ strains that are identical except for the orientation of *cat*. When *cat* is in the same orientation as the operon (NuoG::CM$^+$), transcription is reduced eightfold in comparison to WT, but when *cat* is transcribed opposite (NuoG::CM$^-$) from the *nuo* genes, transcription is down 50-fold (Table 5). That no strains with opposite-orientation *cat* cassettes upstream of Cj1574c could be isolated gives support to the conclusion that expression of Cj1574c is required for viability in *C. jejuni*.

The Cj1574c merodiploid strains. A merodiploid Cj1575c and Cj1574c *C. jejuni* strain was constructed by cloning the coding regions of both into the coding region of *hydA* (Cj1267c). Insertions into *hydA* have no phenotype relevant to these studies, and transcription of *hydA* is constitutive (data not shown), making this a useful locus for unrelated protein expression. The resulting strain (designated 7574MD) contains two copies of Cj1575c and Cj1574c. When 7574MD was used as the parent strain, it was possible to delete a portion of Cj1574c found within the *nuo* operon, yielding Δ74MD. Furthermore, a large deletion of the *nuo* operon could be made, in which *nuoC* to *nuoN* (including Cj1574c and Cj1575c) were deleted and replaced with the *aphA-3* cassette (designated ΔNuoMD [Fig. 1C]). qRT-PCR of WT and ΔNuoMD strains indicates that Cj1574c expression levels are threefold higher in ΔNuoMD than in the WT (Table 5). Δ74MD is unable to grow in MH broth without formate supplementation (Table 4). This result was unexpected, as this strain contains intact copies of all 12 *nuo* genes and is also complemented with Cj1575c and Cj1574c. qRT-PCR assays of *nuoH* in WT and Δ74MD, however, reveal that the *aphA-3* cassette within Cj1574c reduced the expression of downstream genes ~80-fold (Table 5). The requirement for formate in this strain can be attributed to the loss of transcription of *nuoG* to *nuoN*.

Localization of CJ1574. Purified CJ1575 and CJ1574 expressed from *E. coli* were not immune reactive when inoculated into two separate rabbits and did not provide antisera able to identify these proteins (data not shown). We therefore used an epitope-tagged (hexahistidine) version of CJ1574 to create the merodiploid strains. Since this tag has been cloned in frame with Cj1574c, the resulting protein product would

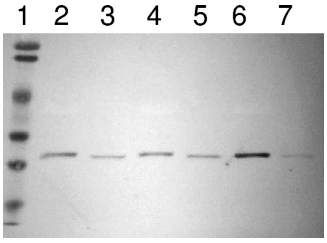

FIG. 3. Immunoblot assay of *C. jejuni* extracts using anti-His primary antibody. Lane 1, prestained low-range standards composed of phosphorylase *b* (113 kDa), bovine serum albumin (92 kDa), ovalbumin (52.3 kDa), carbonic anhydrase (35.3 kDa), soybean trypsin inhibitor (28.7 kDa), and lysozyme (21.3 kDa); lane 2, 7574MD membrane fraction; lane 3, 7475MD soluble fraction; lane 4, Δ74MD membrane fraction; lane 5, Δ74MD soluble fraction; lane 6, ΔNuoMD membrane fraction; lane 7, ΔNuoMD soluble fraction.

contain a hexahistidine epitope tag on the C terminus. Anti-His antibodies recognize an appropriately sized protein expressed in all three strains expressing CJ1574 from the *hyd* operon (Fig. 3). To determine CJ1574 localization, membrane and soluble fractions of each strain were prepared and blotted (Fig. 3). The results indicate that CJ1574 was present in both the membrane and the soluble fractions in all three strains; however, the ratio of membrane-associated protein was highest in strain ΔNuoMD.

Respiratory activities of WT and ΔNuoMD. Respiration rates on various substrates were determined by O_2 uptake using a Clark-type O_2 electrode and CE from WT and ΔNuoMD (Table 6). In agreement with previous studies (8, 14), formate was the preferred substrate for both WT and ΔNuoMD (Table 6). The only substrate tested that was significantly affected by the *nuo* deletion was α-ketoglutarate, a known respiratory substrate in *C. jejuni* (23, 38). WT CE respired α-ketoglutarate at a rate of 16.4 nmol of O_2 consumed minute^{-1} mg of protein^{-1} versus 3.7 nmol of O_2 consumed minute^{-1} mg of protein^{-1} for ΔNuoMD (Table 6). Significantly, *C. jejuni* CE had low rates of respiratory activity with either NADH or NADPH, and these rates were unaffected by the *nuo* deletion (Table 6).

OOR is responsible for α-ketoglutarate respiration in *C. jejuni*. The decreased ability of ΔNuoMD to respire α-ketoglutarate prompted us to look at this substrate as a possible donor to complex I. Previous studies have shown that α-ketoglutarate supports respiration in *C. jejuni* strain 11168 (23) and *C. jejuni* strain ACC 29428 (38); however, the enzymes responsible have not been characterized. We targeted the OorB subunit of the enzyme OOR for mutagenesis by insertion of *cat* into the *oorB* (Cj0537) coding region to yield OorB::CM. CE of OorB::CM displayed negligible α-ketoglutarate and CoA-dependent O_2 uptake (Table 6), indicating that OOR is the sole enzyme responsible for α-ketoglutarate respiration. Furthermore, we were able to show that α-ketoglutarate (plus CoA) initiated the reduction of the electron transport chain, as evidenced by the emergence of peaks at 421 nm, 524 nm, and 553 nm, characteristic of reduced cytochromes. Addition of α-ketoglutarate and CoA to CE of OorB::CM results in no cytochrome reduction, even after a 30-min incubation (data not shown). These data indicate that α-ketoglutarate is oxidized by OOR and that electrons liberated are transferred to O_2 via the respiratory electron transport chain.

Flavodoxin is the electron acceptor of OOR and an essential protein. Attempts to mutate flavodoxin (*fldA*, Cj1382c) in *C. jejuni* were unsuccessful despite many attempts. We used the same strategy to make an *fldA* merodiploid strain as we used with 7574MD, and *fldA* was cloned in frame with a His tag coding sequence into the *hyd* operon, disrupting *hydA* to obtain FldMD. When FldMD was used as the parent strain, we were able to interrupt the original *fldA* gene to obtain FldMD::CM, indicating that flavodoxin is required for viability in *C. jejuni*. A His-tagged version of *C. jejuni* flavodoxin was expressed at high levels in *E. coli* and purified to near homogeneity in one step using nickel-chelate affinity chromatography (Fig. 4A). The recombinant flavodoxin contains a flavin cofactor as determined by visible spectra; however, the nature of the cofactor remains ambiguous. Comparison of purified flavodoxin to a commercially purchased FMN and FAD (Fig. 4B) reveals that although the gross spectra are similar, the absorption maximum for flavodoxin (460 nm) is shifted in relation to both that of FMN (445 nm) and that of FAD (450 nm). Addition of dithionite to the protein leads to reduction of the flavin, which can be monitored by a decrease in absorbance at 460 nm (data not shown). We used the redox state of the flavodoxin to determine if α-ketoglutarate (via OOR) was the electron donor. Purified flavodoxin was incubated with CE of WT and OorB::CM along with α-ketoglutarate and CoA in a stoppered quartz cuvette. Flavodoxin reduction was monitored by a decrease in absorbance of the peak at 460 nm (Fig. 5A). WT CE reduce recombinant flavodoxin at a rate of 213 ± 19 nmol min^{-1} mg of protein^{-1} (Fig. 5A), and OorB::CM CE are unable to reduce flavodoxin (Fig. 5B). These data indicate that in *C. jejuni* (unlike in *H. pylori*) flavodoxin is an efficient electron acceptor of OOR (16). Previous studies have shown that the flavodoxin of *H. pylori* is essential for the survival for this organism (10).

DISCUSSION

In order to fulfill its energy demands, *C. jejuni* relies solely on the respiratory chain and oxidative phosphorylation. Known respiratory substrates for *C. jejuni* include hydrogen, formate, succinate, malate, lactate, sulfite, and α-ketoglutarate (14, 23, 25, 38). Curiously, despite the fact that NADH is a poor respiratory substrate in *C. jejuni* (14), the genome sequence predicts the presence of 12 *nuo* (for *N*ADH *u*biquinone *o*xidoreductase) genes, also called complex I (27). This apparent paradox is explained by the fact that the *nuo* genes that encode

TABLE 6. Respiration rates in strains (CE) with various substrates

Strain	Respiration rate[a] with substrate:			
	Formate	α-Ketoglutarate plus CoA	NADH	NADPH
WT	33.87 ± 19.9	16.43 ± 3.6	2.57 ± 0.25	1.50 ± 0.12
ΔNuoMD	30.83 ± 19.0	3.70 ± 1.3	2.11 ± 0.49	1.56 ± 0.24
OorB::CM	23.67 ± 3.9	0.49 ± 0.32	ND[b]	ND

[a] Rates are expressed as nmoles of O_2 consumed/min/mg of protein.
[b] ND, not determined.

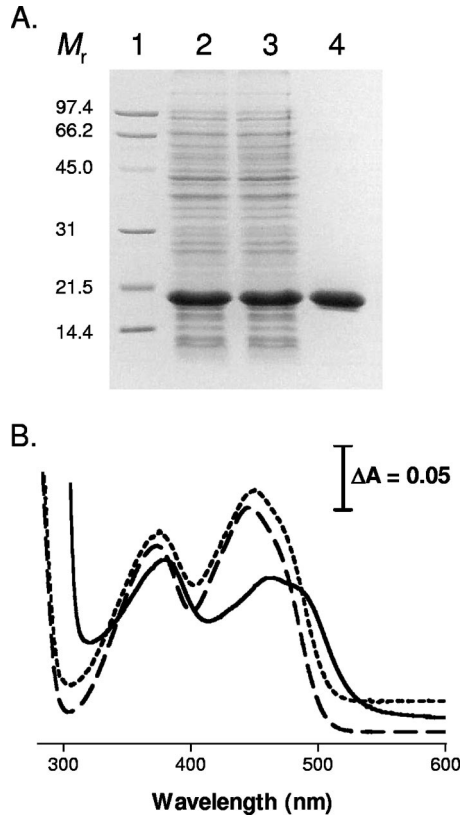

FIG. 4. Purification of flavodoxin. (A) SDS-PAGE. Lane 1, low-range standards (M_r of each standard is to the left of the gel); lane 2, crude extract; lane 3, supernatant of crude extract; lane 4, purified flavodoxin. (B) Absorption spectra of purified flavodoxin (solid line), commercially purchased FMN (dashed line), and commercially purchased FAD (dotted line).

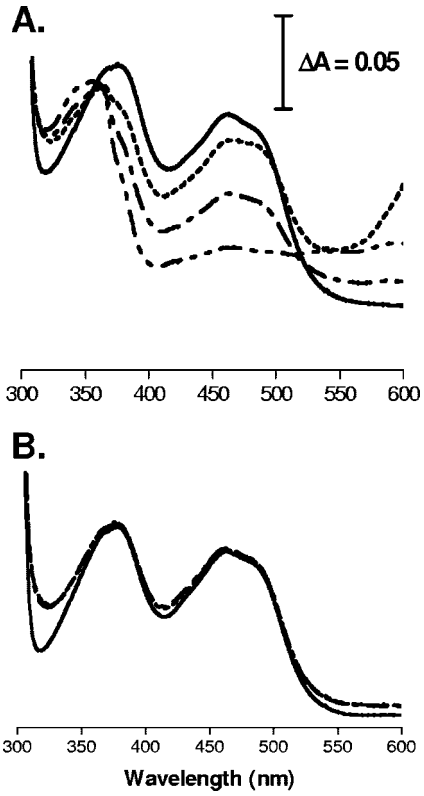

FIG. 5. Reduction of flavodoxin with CE and α-ketoglutarate and CoA. (A) WT CE. Spectrum with no addition (solid line), immediately after the addition of substrates (dashed line), 1 min after the addition of substrates (dashed line with single dots), and 5 min after the addition of substrates (dashed line with double dots). (B) OorB::CM CE. Spectra with no addition (solid line), immediately after the addition of substrates (dashed line), 1 min after the addition of substrates (dashed line with single dots), and 5 min after the addition of substrates (dashed line with double dots).

the NADH dehydrogenase module subunits (*nuoE* and *nuoF*) are absent from the operon. In the place of *nuoE* and *nuoF* (between *nuoD* and *nuoG* [Fig. 1A]) are two novel genes, Cj1574c and Cj1575c. We present a model (Fig. 6) whereby these novel proteins act as electron acceptors from a flavodoxin rather than NADH. In this model flavodoxin acts (like NADH) as an intermediate between central carbon metabolism and the electron transport chain.

Despite the lack of NADH dehydrogenase activity, *C. jejuni* complex I is a major point of entry of electrons into the respiratory chain. *nuo* mutants fail to grow in MH broth, but growth can be restored when provided with an alternative respiratory substrate such as formate (Table 4). In contrast to the 12 *nuo* genes, Cj1574c (the sixth gene of the *nuo* operon [Fig. 1A]) is essential for viability of *C. jejuni*. We draw this conclusion based on three criteria. First, repeated attempts to interrupt or delete the gene via allelic replacement were unsuccessful, despite the ability to interrupt or delete the other 12 genes of the operon. Second, genes "upstream" of Cj1574c can be interrupted only when the drug cassette is in an orientation that allows transcription of downstream genes. Third, when a second copy of Cj1574c was provided on a second location in the genome (a Cj1574c merodiploid), the entire *nuo* operon was dispensable.

Strain ΔNuoMD contains a large (10.5-kb) deletion from the middle of *nuoC* to the beginning of *nuoN* (Fig. 1C). Importantly, Cj1574c is expressed in this strain from the inserted copy both transcriptionally (Table 5) and translationally (as measured by immunoblotting [Fig. 3]). We used this strain to identify the physiological donor to complex I. Respiratory activities (as measured by O_2 uptake) were similar to those of the parent strain for all respiratory substrates tested except for

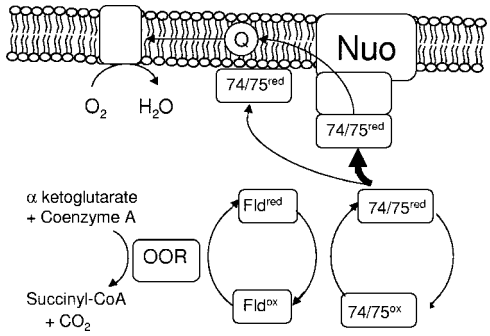

FIG. 6. Model of the *C. jejuni* respiratory pathway through complex I. Arrows indicate the flow of electrons.

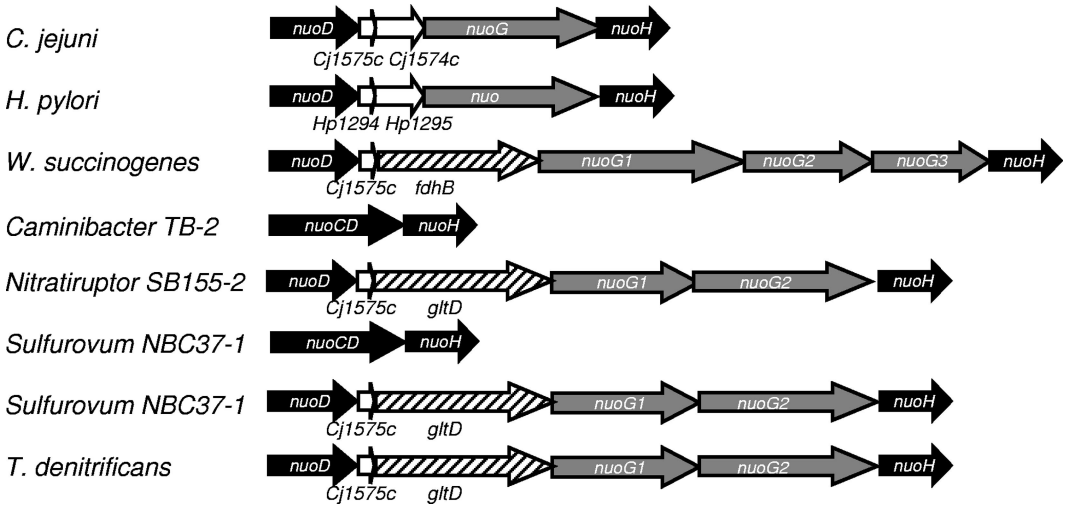

FIG. 7. Genetic organization of the *nuo* operons from various *Epsilonproteobacteria*. Only the regions between *nuoD* and *nuoH* are shown; each bacterium also encodes *nuoA* to *nuoC* and *nuoI* to *nuoN*. References for each genome sequence are in parentheses: *C. jejuni* (27), *H. pylori* (34), *Wolinella succinogenes* (2), *Caminibacter mediatlanticus* TB-2 (C. Vetriani, S. Ferriera, J. Johnson, S. Kravitz, K. Beeson, G. Sutton, Y.-H. Rogers, R. Friedman, M. Frazier, and J. C. Venter, direct submission to EMBL/GenBank/DDBJ, 2007), *Nitratiruptor* strain SB155-2 and the two operons from *Sulfurovum* strain NBC37-1 (26), and *Thiomicrospira denitrificans* ATCC 33889 (A. Copeland, S. Lucas, A. Lapidus, K. Barry, J. C. Detter, T. Glavina, N. Hammon, S. Israni, S. Pitluck, P. Chain, S. Malfatti, M. Shin, L. Vergez, J. Schmutz, F. Larimer, M. Land, N. Kyrpides, A. Lykidis, and P. Richardson, unpublished data).

α-ketoglutarate (Table 6). α-Ketoglutarate is a tricarboxylic acid (TCA) cycle intermediate and the entry point for many amino acids into central carbon metabolism, making it especially important in an asaccharolytic organism such as *C. jejuni* that garners most of its carbon and energy from amino acids (18, 22, 35). OOR (encoded by *oorDABC* [Cj0535 to Cj0538]) is a functional equivalent to α-ketoglutarate dehydrogenase in that it catalyzes the decarboxylation of α-ketoglutarate to form succinyl-CoA (16). The OOR mutant strain supports neither α-ketoglutarate-dependent cytochrome reduction nor α-ketoglutarate-dependent O_2 uptake (Table 6). Although the oxidative TCA cycle is interrupted in OorB::CM, the mutation is not lethal due to the presence of reductive TCA enzymes (e.g., fumarate reductase) which allow for the synthesis of important biosynthetic precursors. One major difference between OOR and α-ketoglutarate dehydrogenase is that the reducing equivalents from OOR are transferred to a low-potential protein electron acceptor rather than NADH. In search of the physiological electron acceptor to OOR, we mutated two ferredoxin genes (Cj0333c and Cj0369c) and found no effect on α-ketoglutarate respiratory activity (data not shown). Attempts to mutate the *C. jejuni* flavodoxin gene (*fldA*) proved unsuccessful unless a second copy of *fldA* was provided on the chromosome. We conclude that *fldA* (like Cj1574c) is an essential gene in *C. jejuni*. Flavodoxin has also been shown to be essential in *H. pylori* (10). *C. jejuni* flavodoxin expressed heterologously in *E. coli* and purified by nickel chelate affinity chromatography (Fig. 4A) contains a flavin cofactor that can be monitored spectrophotometrically (Fig. 4B). Extracts of WT *C. jejuni* reduce flavodoxin when provided with α-ketoglutarate and CoA (Fig. 5A); extracts of OorB::CM do not (Fig. 5B). These data indicate that the electron acceptor for OOR in *C. jejuni* is flavodoxin, in contrast to *H. pylori*, where the electron acceptor was determined not to be flavodoxin (16).

Taken together, these data indicate that complex I in *C. jejuni* is an entry point for electrons into the respiratory electron transport chain from a reduced flavodoxin. We also conclude that CJ1574 (and possibly CJ1575, but we will speculate only on CJ1574 here) is required for viability of *C. jejuni* and involved in both electron transport and flavodoxin redox cycling. In our model (Fig. 6), we believe that in WT cells CJ1574 is part of complex I and facilitates the transfer of electrons into the complex. Furthermore, in the absence of a functional complex I (such is the case in all the *nuo* mutants), CJ1574 retains its role in facilitating the oxidation of flavodoxin. This model explains why CJ1574 is essential, as without this activity the flavodoxin pool would remain reduced. Oxidized flavodoxin is required for the activity of both OOR and PFOR (15, 31), both of which are important enzymes of central carbon metabolism. The importance of a pool of oxidized flavodoxin is indicated by the essential nature of both flavodoxin and CJ1574.

O_2 is the final electron acceptor of flavodoxin regardless of whether complex I is intact. Although greatly reduced, the *nuo* deletion strain retains partial α-ketoglutarate-dependent O_2 uptake activity (Table 6), and CJ1574 is still membrane associated (Fig. 3). We conclude that this low level of CJ1574-mediated electron flow in the *nuo* mutants is sufficient to provide a pool of oxidized flavodoxin but does not provide enough energy to support growth of the cultures in the absence of formate (Table 4). A recent study has shown that in *H. pylori* flavodoxin interacts with a flavin quinone reductase that the authors termed FqrB (31). FqrB was shown to mediate the transfer of electrons from flavodoxin to NADP to form NADPH. FqrB is also present in *C. jejuni* and can accept electrons from reduced flavodoxin (31). Although we feel it most likely that CJ1574 and FqrB accept electrons from flavodoxin independently, we cannot rule out the possibility that FqrB is an intermediate in electron flow from flavodoxin to the

respiratory chain. We do not believe, however, that NADPH is involved in the electron transfer to the respiratory chain. The level of NADPH-dependent respiratory activity observed (Table 6) is too low to account for the rate of α-ketoglutarate-dependent O_2 uptake.

C. jejuni belongs to the epsilon class of the proteobacteria, the diversity of which has only recently been recognized. In addition to the well-studied pathogens of the genera *Campylobacter* and *Helicobacter*, the *Epsilonproteobacteria* also include many marine and terrestrial aquatic species (7) and may be the dominant bacterial species in deep-sea hydrothermal vent systems (33). Abandoning the NADH dehydrogenase module form appears to be an early event in the evolution of the *Epsilonproteobacteria*, as *nuoE* and *nuoF* are absent from all epsilonproteobacterial genome sequences, despite the presence of *nuo* operons (Fig. 7). Three different strategies have been employed by these bacteria to cope with the loss of *nuoE* and *nuoF*: replacement with Cj1575c and Cj1574c homologues (as in *Campylobacter* and *Helicobacter* species), deletion (along with *nuoG*) without replacement (as in *Caminibacter mediatlanticus* TB-2 and one of the *Sulfurovum* strain NBC37-1 operons), and duplication of *nuoG* and recruitment of a Cj1575c homologue and either *gltD* or *fdhB* (as in *Wolinella succinogenes*, *Nitratiruptor* strain SB155-2, *Thiomicrospira denitrificans* ATCC 33889, and one of the *Sulfurovum* strain NBC37-1 operons) (Fig. 7). The different strategies employed by the *Epsilonproteobacteria* likely reflect the different needs of each bacterium adapted to its specific environment. The ε-proteobacters of the hydrothermal vent systems grow autotrophically using the reductive TCA cycle to fix CO_2 and relying heavily on inorganics for energy (7, 32). The presence of the reversible enzymes PFOR and OOR (both of which are required for the reductive TCA cycle) in the *Epsilonproteobacteria* is likely the legacy of this autotrophic lifestyle (32). *C. jejuni*, on the other hand, thrives in the resource-rich environment of the animal intestinal tract and employs an oxidative TCA cycle to garner energy from organic compounds found in its ecological niche. In this evolutionary context, the adaptation of complex I to accept electrons from flavodoxin is a logical response to inheriting a TCA cycle that employs PFOR and OOR. A better understanding of this unusual respiratory pathway (at least two of the components of which are essential for *C. jejuni* viability) could prove vital in devising strategies to eliminate this important human pathogen from the food supply.

ACKNOWLEDGMENTS

This work was supported by USDA-NRI grant 2004-04553.

We thank Debbie Threadgill and Jay Andrus for the kind gift of pJMA-001.

REFERENCES

1. **Altekruse, S. F., N. J. Stern, P. I. Fields, and D. L. Swerdlow.** 1999. *Campylobacter jejuni*—an emerging foodborne pathogen. Emerg. Infect. Dis. **5:**28–35.
2. **Baar, C., M. Eppinger, G. Raddatz, J. Simon, C. Lanz, O. Klimmek, R. Nandakumar, R. Gross, A. Rosinus, H. Keller, P. Jagtap, B. Linke, F. Meyer, H. Lederer, and S. C. Schuster.** 2003. Complete genome sequence and analysis of *Wolinella succinogenes*. Proc. Natl. Acad. Sci. USA **100:**11690–11695.
3. **Beery, J. T., M. B. Hugdahl, and M. P. Doyle.** 1988. Colonization of gastrointestinal tracts of chicks by *Campylobacter jejuni*. Appl. Environ. Microbiol. **54:**2365–2370.
4. **Braun, M., S. Bungert, and T. Friedrich.** 1998. Characterization of the overproduced NADH dehydrogenase fragment of the NADH:ubiquinone oxidoreductase (complex I) from *Escherichia coli*. Biochemistry **37:**1861–1867.
5. **Bruschi, M., and F. Guerlesquin.** 1988. Structure, function and evolution of bacterial ferredoxins. FEMS Microbiol. Rev. **4:**155–175.
6. **Butzler, J. P.** 2004. *Campylobacter*, from obscurity to celebrity. Clin. Microbiol. Infect. **10:**868–876.
7. **Campbell, B. J., A. S. Engel, M. L. Porter, and K. Takai.** 2006. The versatile epsilon-proteobacteria: key players in sulphidic habitats. Nat. Rev. Microbiol. **4:**458–468.
8. **Carlone, G. M., and J. Lascelles.** 1982. Aerobic and anaerobic respiratory systems in *Campylobacter fetus* subsp. *jejuni* grown in atmospheres containing hydrogen. J. Bacteriol. **152:**306–314.
9. **Finel, M.** 1998. Does NADH play a central role in energy metabolism in *Helicobacter pylori*? Trends Biochem. Sci. **23:**412–413.
10. **Freigang, J., K. Diederichs, K. P. Schafer, W. Welte, and R. Paul.** 2002. Crystal structure of oxidized flavodoxin, an essential protein in *Helicobacter pylori*. Protein Sci. **11:**253–261.
11. **Friedman, C. R., J. Neiman, H. C. Wegener, and R. V. Tauxe.** 2000. Epidemiology of *Campylobacter jejuni* in the United States and other industrialized nations, p. 121–138. *In* I. Nachamkin and M. J. Blaser (ed.), *Campylobacter*, 2nd ed. ASM Press, Washington, DC.
12. **Friedrich, T., and B. Bottcher.** 2004. The gross structure of the respiratory complex I: a Lego system. Biochim. Biophys. Acta **1608:**1–9.
13. **Friedrich, T., and D. Scheide.** 2000. The respiratory complex I of bacteria, archaea and eukarya and its module common with membrane-bound multisubunit hydrogenases. FEBS Lett. **479:**1–5.
14. **Hoffman, P. S., and T. G. Goodman.** 1982. Respiratory physiology and energy conservation efficiency of *Campylobacter jejuni*. J. Bacteriol. **150:**319–326.
15. **Hughes, N. J., P. A. Chalk, C. L. Clayton, and D. J. Kelly.** 1995. Identification of carboxylation enzymes and characterization of a novel four-subunit pyruvate:flavodoxin oxidoreductase from *Helicobacter pylori*. J. Bacteriol. **177:**3953–3959.
16. **Hughes, N. J., C. L. Clayton, P. A. Chalk, and D. J. Kelly.** 1998. *Helicobacter pylori porCDAB* and *oorDABC* genes encode distinct pyruvate:flavodoxin and 2-oxoglutarate:acceptor oxidoreductases which mediate electron transport to NADP. J. Bacteriol. **180:**1119–1128.
17. **Laemmli, U. K.** 1970. Cleavage of structural proteins during the assembly of the head of bacteriophage T4. Nature **227:**680–685.
18. **Leach, S., P. Harvey, and R. Wali.** 1997. Changes with growth rate in the membrane lipid composition of and amino acid utilization by continuous cultures of *Campylobacter jejuni*. J. Appl. Microbiol. **82:**631–640.
19. **Leif, H., V. D. Sled, T. Ohnishi, H. Weiss, and T. Friedrich.** 1995. Isolation and characterization of the proton-translocating NADH: ubiquinone oxidoreductase from *Escherichia coli*. Eur. J. Biochem. **230:**538–548.
20. **Lu, J., U. Idris, B. Harmon, C. Hofacre, J. J. Maurer, and M. D. Lee.** 2003. Diversity and succession of the intestinal bacterial community of the maturing broiler chicken. Appl. Environ. Microbiol. **69:**6816–6824.
21. **Mead, P. S., L. Slutsker, V. Dietz, L. F. McCaig, J. S. Bresee, C. Shapiro, P. M. Griffin, and R. V. Tauxe.** 1999. Food-related illness and death in the United States. Emerg. Infect. Dis. **5:**607–625.
22. **Mendz, G. L., G. E. Ball, and D. J. Meek.** 1997. Pyruvate metabolism in *Campylobacter* spp. Biochim. Biophys. Acta **1334:**291–302.
23. **Mohammed, K. A., R. J. Miles, and M. A. Halablab.** 2004. The pattern and kinetics of substrate metabolism of *Campylobacter jejuni* and *Campylobacter coli*. Lett. Appl. Microbiol. **39:**261–266.
24. **Myers, J. D., and D. J. Kelly.** 2005. Respiratory electron transport in *Helicobacter* and *Campylobacter*, p. 63–80. *In* D. Zannoni (ed.), Respiration in archaea and bacteria, vol. 2. Diversity of prokaryotic respiratory systems. Kluwer Academic Publishers, Dordrecht, The Netherlands.
25. **Myers, J. D., and D. J. Kelly.** 2005. A sulphite respiration system in the chemoheterotrophic human pathogen *Campylobacter jejuni*. Microbiology **151:**233–242.
26. **Nakagawa, S., Y. Takaki, S. Shimamura, A. L. Reysenbach, K. Takai, and K. Horikoshi.** 2007. Deep-sea vent ε-proteobacterial genomes provide insights into emergence of pathogens. Proc. Natl. Acad. Sci. USA **104:**12146–12150.
27. **Parkhill, J., B. W. Wren, K. Mungall, J. M. Ketley, C. Churcher, D. Basham, T. Chillingworth, R. M. Davies, T. Feltwell, S. Holroyd, K. Jagels, A. V. Karlyshev, S. Moule, M. J. Pallen, C. W. Penn, M. A. Quail, M. A. Rajandream, K. M. Rutherford, A. H. van Vliet, S. Whitehead, and B. G. Barrell.** 2000. The genome sequence of the food-borne pathogen *Campylobacter jejuni* reveals hypervariable sequences. Nature **403:**665–668.
28. **Pieulle, L., M. H. Charon, P. Bianco, J. Bonicel, Y. Petillot, and E. C. Hatchikian.** 1999. Structural and kinetic studies of the pyruvate-ferredoxin oxidoreductase/ferredoxin complex from *Desulfovibrio africanus*. Eur. J. Biochem. **264:**500–508.
29. **Sancho, J.** 2006. Flavodoxins: sequence, folding, binding, function and beyond. Cell. Mol. Life Sci. **63:**855–864.
30. **Smith, M. A., M. Finel, V. Korolik, and G. L. Mendz.** 2000. Characteristics

of the aerobic respiratory chains of the microaerophiles *Campylobacter jejuni* and *Helicobacter pylori*. Arch. Microbiol. **174:**1–10.

31. **St. Maurice, M., N. Cremades, M. A. Croxen, G. Sisson, J. Sancho, and P. S. Hoffman.** 2007. Flavodoxin:quinone reductase (FqrB): a redox partner of pyruvate:ferredoxin oxidoreductase that reversibly couples pyruvate oxidation to NADPH production in *Helicobacter pylori* and *Campylobacter jejuni*. J. Bacteriol. **189:**4764–4773.
32. **Takai, K., B. J. Campbell, S. C. Cary, M. Suzuki, H. Oida, T. Nunoura, H. Hirayama, S. Nakagawa, Y. Suzuki, F. Inagaki, and K. Horikoshi.** 2005. Enzymatic and genetic characterization of carbon and energy metabolisms by deep-sea hydrothermal chemolithoautotrophic isolates of *Epsilonproteobacteria*. Appl. Environ. Microbiol. **71:**7310–7320.
33. **Takai, K., H. Oida, Y. Suzuki, H. Hirayama, S. Nakagawa, T. Nunoura, F. Inagaki, K. H. Nealson, and K. Horikoshi.** 2004. Spatial distribution of marine crenarchaeota group I in the vicinity of deep-sea hydrothermal systems. Appl. Environ. Microbiol. **70:**2404–2413.
34. **Tomb, J. F., O. White, A. R. Kerlavage, R. A. Clayton, G. G. Sutton, R. D. Fleischmann, K. A. Ketchum, H. P. Klenk, S. Gill, B. A. Dougherty, K. Nelson, J. Quackenbush, L. Zhou, E. F. Kirkness, S. Peterson, B. Loftus, D. Richardson, R. Dodson, H. G. Khalak, A. Glodek, K. McKenney, L. M. Fitzegerald, N. Lee, M. D. Adams, E. K. Hickey, D. E. Berg, J. D. Gocayne, T. R. Utterback, J. D. Peterson, J. M. Kelley, M. D. Cotton, J. M. Weidman, C. Fujii, C. Bowman, L. Watthey, E. Wallin, W. S. Hayes, M. Borodovsky, P. D. Karp, H. O. Smith, C. M. Fraser, and J. C. Venter.** 1997. The complete genome sequence of the gastric pathogen *Helicobacter pylori*. Nature **388:** 539–547.
35. **Velayudhan, J., M. A. Jones, P. A. Barrow, and D. J. Kelly.** 2004. L-Serine catabolism via an oxygen-labile L-serine dehydratase is essential for colonization of the avian gut by *Campylobacter jejuni*. Infect. Immun. **72:**260–268.
36. **Wang, Y., and D. E. Taylor.** 1990. Chloramphenicol resistance in *Campylobacter coli*: nucleotide sequence, expression, and cloning vector construction. Gene **94:**23–28.
37. **Weidner, U., S. Geier, A. Ptock, T. Friedrich, H. Leif, and H. Weiss.** 1993. The gene locus of the proton-translocating NADH:ubiquinone oxidoreductase in *Escherichia coli*. Organization of the 14 genes and relationship between the derived proteins and subunits of mitochondrial complex I. J. Mol. Biol. **233:**109–122.
38. **Westfall, H. N., D. M. Rollins, and E. Weiss.** 1986. Substrate utilization by *Campylobacter jejuni* and *Campylobacter coli*. Appl. Environ. Microbiol. **52:** 700–705.
39. **Yagi, T.** 1986. Purification and characterization of NADH dehydrogenase complex from *Paracoccus denitrificans*. Arch. Biochem. Biophys. **250:**302–311.
40. **Yano, T., S. S. Chu, V. D. Sled, T. Ohnishi, and T. Yagi.** 1997. The proton-translocating NADH-quinone oxidoreductase (NDH-1) of thermophilic bacterium *Thermus thermophilus* HB-8. Complete DNA sequence of the gene cluster and thermostable properties of the expressed NQO2 subunit. J. Biol. Chem. **272:**4201–4211.
41. **Yao, R., R. A. Alm, T. J. Trust, and P. Guerry.** 1993. Construction of new *Campylobacter* cloning vectors and a new mutational *cat* cassette. Gene **130:**127–130.